Consequence of shape elongation on emission asymmetry for colloidal CdSe/CdS nanoplatelets

Fu Feng[1], Loan Thu NGuyen[1,2], Michel Nasilowski[3], Brice Nadal[3], Benoît Dubertret[3], Laurent Coolen[1], and Agnès Maître[1] (✉)

[1] *Sorbonne Universités, UPMC Univ Paris 06, CNRS-UMR 7588, Institut des NanoSciences de Paris, F-75005 Paris, France*

[2] *Institute of Materials Science, Vietnam Academy of Science and Technology, 18 Hoang Quoc Viet Road, Cau Giay Dist., 100000 Hanoi, Vietnam*

[3] *Laboratoire de Physique et d'Etude des Matériaux, ESPCI, UPMC Univ Paris 6, CNRS, 10 rue Vauquelin, F-75005 Paris, France*

ABSTRACT

In this paper, we demonstrate that for colloidal CdSe/CdS nanoplatelets, a rectangular shape induces emission asymmetry, in terms of both polarization and emission patterns. Polarimetry and emission pattern analyses are combined to provide information on the orientation of the transition dipoles involved in the nanoplatelet emission. It is shown that for rectangular nanoplatelets, the emission is polarized and the emission patterns are anisotropic, whereas they remain nonpolarized and isotropic for square nanoplatelets. This can be appropriately described by the dielectric antenna effect induced by the elongated shape of the rectangular platelet.

KEYWORDS

colloidal semiconductor nanoplatelet,
emission dipole,
emission polarization,
emission pattern

1 Introduction

Understanding the photophysics of fluorescent semiconductor nanostructures is of crucial importance for their integration in lighting, displays, or photovoltaic devices. Their fluorescent emission usually exhibits a degree of polarization, whose enhancement is crucial for many devices. Polarization depends on three characteristics: the dielectric environment of the emitter, the orientation of the emitter, and the symmetry of the emitting states. Some fluorescent nanoemitters behave as single linear dipoles, often referred to as "one-dimensional (1D) dipoles". However, the emission in many such nanoemitters originates from the degenerate states of different symmetries. Referred to as "two-dimensional (2D) dipoles" they behave as an incoherent sum of two orthogonal linear dipoles with the same oscillator strengths [1]. In both cases,

Address correspondence to agnes.maitre@insp.upmc.fr

polarized emission can be observed, with the degree of polarization depending of their orientation (with polarization degree higher for 1D dipoles). Analyses using polarimetric methods, sometimes combined with defocused imaging or decay curves, have demonstrated 2D-dipole behavior for spherical core–shell quantum dots [1–4] and dot-in-plate structures [5], and 1D-dipole behavior for nanorods [6] and dot-in-rods [7], with intermediate 1D+2D behavior for some structures [8, 9]. These studies have found dipolar nature (1D or 2D) to be related both to the symmetry and degeneracy of the electron–hole transition dipole, and also to the shape of the nano-object, even when the Bohr radius of the exciton is smaller than the size of the nano-object, a size difference that should made the dipolar transition insensitive to spatial confinement. A relationship between shape and polarized radiation has been shown, in particular, for colloidal dot-in-rods, and has sometimes been interpreted as a dielectric antenna effect of the rod-like shell [7, 9–12]. This has also been observed for nanowires [13] and porous silicon [14].

Researchers have recently synthesized flat colloidal CdSe nanoplatelets of a few atomic monolayers arranged in a zinc blende structure [15, 16]. These nanoplatelets exhibit behavior analogous to semiconductor quantum wells [17]. Their synthesis is controlled with atomic precision, and they exhibit a fluorescence emission line width close to $k_B T$ at room temperature [18–20]. The overgrowth of a shell (typically of a wider band gap such as CdS or ZnS on CdSe) on the core material has been proven as an efficient way for 1) increasing both the quantum yield and stability of the emitters, and 2) decreasing their emission blinking [21–25]. The luminescence dynamics have been studied, for example, as a function of the lateral dimensions of the nanoplatelets [26–29], and partial emission polarization has been found for elongated platelets [30, 31]. However, the dipolar nature of these emitters has not yet been investigated.

It will depend on electron–hole quantum confinement, but also on the platelet dielectric confinement that acts on electron–hole radiation [32, 33]. Additionally, it could be modified by ligands, local fluctuations, trap states, etc. [34].

The objective of this study is to demonstrate how nanoplatelet shapes can induce anisotropic emission, which addresses both an increase in the degree of polarization and asymmetric radiation pattern. To achieve this, we compare individual square and rectangular nanoplatelets, and their emission properties (in terms of polarization and emission patterns). The dipole characteristics of individual CdSe/CdS nanoplatelets are investigated, and a correlation between the spatial anisotropy of the nanoplatelets, their polarized emissions, and the asymmetry of their radiation patterns is evidenced. By using an appropriate substrate and analyzing polarization and radiation patterns, the emitting dipole nature and other characteristics of square and rectangle nanoplatelet emissions are unambiguously determined.

2 Experimental

The CdSe/CdS core–shell nanoplatelets studied here are nanoparticles that have perfectly defined and controlled thicknesses, but whose lateral sizes can be tuned [35]. This allows rectangular and square core/shell nanoplatelets to be synthetized (this synthesis is described in the Electronic Supplementary Material (ESM)).

Figure 1(a) shows transmission electron microscopy (TEM) images of two samples of interest. Both are flat nanoplatelets with a central CdSe layer (1.2 nm thickness) sandwiched between two shell CdS layers (0.4 nm thickness) for a total thickness of 2 nm. For the first sample, the platelets are squares of typical lateral dimensions of 16 nm × 16 nm (+/– 2 nm). For the second sample, the platelets are rectangles with typical lateral dimensions of 15 nm × 20 nm (+/– 3 nm). A spatial anisotropy factor τ is defined as $\frac{\text{length}}{\text{width}} = \frac{1+\tau}{1-\tau}$. This factor τ ranges between 0 (square platelet) and 1 (very elongated rectangle). The values extracted from the TEM images (Fig. 1(b)) are very low for the square platelets (between 0 and 0.08), corresponding to very slight elongation for these structures. For the rectangle sample, on the other hand, the shape anisotropy τ values range between 0.1 and 0.25, indicating a clear rectangular shape.

A microphotoluminescence setup has been used to analyze the fluorescence from individual nanoplatelets

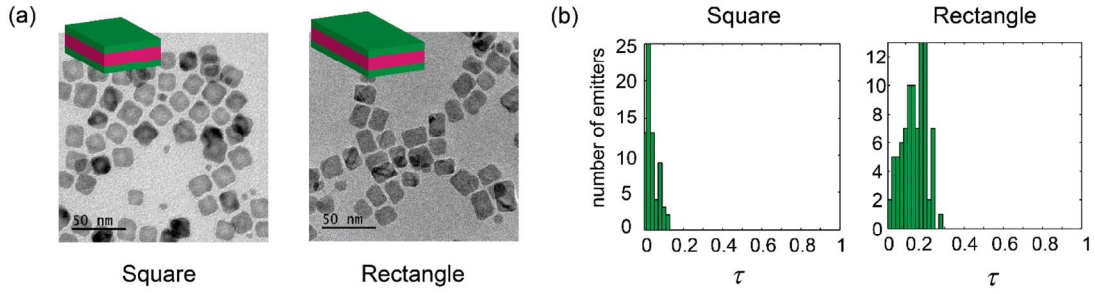

Figure 1 (a) TEM images of the square and rectangle nanoplatelets. (b) Histogram of anisotropic factor τ for square and rectangle nanoplatelets.

deposited on a gold–silica substrate (see the ESM). We excite each single nano-object at a wavelength of 450 nm, very far from the gap wavelength at room temperature. Therefore, different emitting transitions will be considered to be incoherent. For each emitter, we apply two complementary emission analyses: a polarimetry analysis and an angular distribution measurement (radiation pattern). As we describe below, it is necessary to combine these two methods in order to unambiguously determine the following characteristics: 1) the 1D or 2D nature of the emitting dipole and 2) its orientation (Θ, Φ) (in spherical coordinates, with the main axis being normal to the substrate). In the case of 2D dipoles, for CdSe/CdS, the two incoherent σ^+ and σ^- transitions will be described, by a change of basis, as the sum of two linear orthogonal incoherent emitting dipoles. The orientation (Θ, Φ) of the 2D dipole is then normal to the plane containing the two orthogonal linear transitions (or the two σ^+ and σ^- transitions). As described in [4, 7, 36], a linear polarization analysis allows us to retrieve information regarding the nature and orientation of the emitting dipole.

For a 1D dipole, in a polarimetry emission analysis [4], the intensity of the emission transmitted by a rotating polarizer along angle α can be expressed as $I(\alpha) = I_{min} + (I_{max} - I_{min})\cos^2(\Phi - \alpha)$ (Eq. (1)). The value of Φ yields the azimuthal (in-plane) orientation of the dipole. The degree of polarization is defined as $\delta = (I_{max} - I_{min})/(I_{max} + I_{min})$, with its value depending on the measurement conditions (substrate index, objective numerical aperture…) and on the zenithal (out-of-plane) orientation Θ of the dipole. Such a relationship can also be demonstrated in the case of a 2D dipole (see the ESM). Figure 2(c) shows the calculated $\delta(\Theta)$ for 1D and 2D dipoles placed inside a homogeneous medium of index 1.45 at a distance of 50 nm from a 200 nm thick layer of gold, the emission being collected by an oil objective with a numerical aperture of 1.4. The theoretical value of δ is a bijective function of Θ, making it possible to precisely determine Θ from the value of δ, provided that it is known *a priori* whether the dipole is 1D or 2D.

In sections 3.1 and 3.2, the radiation pattern of a nanoplatelet is calculated by describing it as a point-like dipole close to an interface and embedded in a dielectric medium of infinite lateral dimension, following an analytical approach based on interferences between the propagating fields directly emitted, transmitted, or reflected on interfaces [37, 38]. In the former experimental configuration, the radiation pattern calculated for 1D and 2D dipoles with $\Theta = 0°$ are plotted in Fig. 2(d) as a function of the emission directions referred to as (θ, φ) in the spherical coordinates. In section 3.3, we will use a full 3D numerical approach to account for the finite size of the nanoplatelets.

3 Results and discussion

3.1 Square platelets: symmetric and nonpolarized emission from a single 2D-dipole

Figure 2(a) plots an experimental polarimetry curve $I(\alpha)$ for a single square platelet, using the experimental conditions described in the previous section. This curve is appropriately fit by Eq. (1) with a polarization degree of $\delta = 0.02$. By repeating this measurement for 20 emitters (Fig. 2(b)), the measured values of δ are distributed about an average of 0.03, with a standard

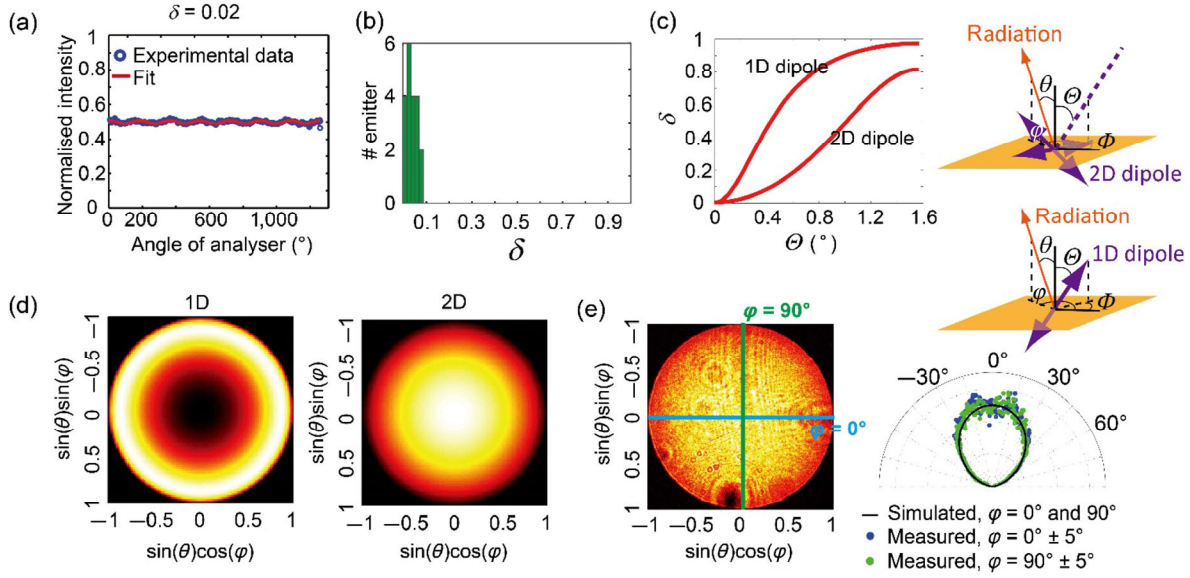

Figure 2 (a) Measured emission polarization curve for a square nanoplatelet. (b) Histogram of measured degrees of polarization for 20 different square nanoplatelets. (c) Theoretical curve of emission degree of polarization with respect to dipole orientation Θ for 1D and 2D dipoles (dipoles lying on a silica plane surface at a distance of 50 nm from a thick gold layer, embedded in a semi-infinite 1.5 index medium and emission collected with an oil objective of numerical aperture NA = 1.4); the schematics show the definition of radiation direction (angles (θ, φ)) and of dipole orientation (angles (Θ, Φ) referring to the dipole orientation for a 1D dipole and to the orientation normal to the dipole plane for a 2D dipole). (d) Calculated radiation pattern in the same configuration for a 1D dipole (left) and 2D dipole (right) at $\Theta = 0°$. (e) Left: measured radiation pattern for an individual square nanoplatelet; right: detailed comparison between the calculated radiation patterns along orthogonal directions at $\varphi = 0°$ and 90° (black curve) and measured radiation patterns at $\varphi = 0°$ (blue dots) and $\varphi = 90°$ (green dots).

deviation of 0.02. Therefore, the emission for each square nanoplatelet are nearly unpolarized, indicating an emitter with revolution symmetry about the z axis. The emission from an individual square nanoplatelet can be described either by a 1D dipole with $\Theta \approx 0°$ (vertical dipole), or by a 2D dipole with $\Theta \approx 0°$ (two horizontal dipoles). Both situations are expected to lead to nonpolarized collected light ($\delta \approx 0$), as shown on the theoretical curve $\delta(\Theta)$ (Fig. 2(c)). At this point, polarimetric measurement does not allow for this ambiguity to be clarified.

To discriminate between 1D and 2D dipoles, the emission for the same platelet is imaged onto an EMCCD camera in the Fourier plane, which provides the radiation pattern of the emitter (see the ESM). The theoretical radiation patterns (Fig. 2(d)) are significantly different between 1D and 2D dipoles of orientation $\Theta = 0°$. The emission of the 2D dipole is maximum at the center ($\theta = 0°$), but minimal for the 1D dipole. This behavior raises the possibility of determining whether the platelets are 1D or 2D dipoles. The measured radiation pattern (Fig. 2(e)) is in qualitative agreement with the calculated radiation pattern from a 2D dipole at $\Theta = 0°$, and significantly differs from the pattern of a 1D dipole. Figure 2(f) shows quantitatively excellent agreement between the measured and calculated radiation patterns. For all of the individual nanoplatelets, all of the radiation patterns exhibited the same diagram (see Fig. S4 in the ESM). This leads to the conclusion that the emission from a square nanoplatelet is very well described by a 2D dipole at $\Theta = 0°$, corresponding to a deterministic deposition of the 2D dipole horizontally on the substrate.

Indeed, the 2D dipolar emission is in agreement with the behavior expected from an ideal thin quantum well. For such very thin structures, quantum confinement along the vertical dimension strongly separates light and heavy holes, so that fluorescence originates only from the recombination of the heavy hole with the electron [15]. Electron-heavy-hole pairs have ±1 or ±2 angular momentums [39]. Only the

degenerate ±1 transitions are optically allowed and contribute to emission at room temperature [26]. Because an incoherent sum of ±1 states is equivalent to a sum of incoherent orthogonal linear dipoles, colloidal nanoplatelets can thus be expected to be pure 2D-dipole emitters, as confirmed by the present experiment.

3.2 Rectangular nanoplatelets, and asymmetric and polarized emission from a single asymmetric 2D-dipole

For square nanoplatelets, both the degree of polarization δ and the spatial anisotropy τ are close to but not always strictly equal to 0 (Figs. 1(b) and 2(b)). To evaluate the relationship between spatial anisotropy and polarized emission, the same experiments are performed on the rectangle nanoplatelets, which have a much larger spatial anisotropy factor than the square nanoplatelets (Fig. 1(b)).

The degree of polarization δ measured for 29 rectangular platelets (Fig. 3(a)), now ranges between 10% and 30%, which is much higher than the polarization for the square nanoplatelets, suggesting a correlation between the degree of polarization and the shape anisotropy of the rectangular nanoplatelets. This relatively high degree of polarization can be explained by two different hypotheses: (i) for a horizontal 2D dipole ($\Theta = 0$), because of the shape anisotropy, one component of the 2D dipole is enhanced with respect to the other (asymmetric 2D dipole), (ii) or the 2D dipole is tilted by an angle $\Theta \neq 0$ (without any dipole asymmetry), possibly because of the nonuniform distribution of ligands around the semi-conductor structure.

Hypothesis (i) can be modeled as the emission of two incoherent dipoles along the horizontal x and y directions, with different dipole moments d_x and d_y. This dipolar asymmetry will be expressed as $\left\|\frac{d_x}{d_y}\right\|^2 = \frac{1+\eta}{1-\eta}$, so that the dipole asymmetry factor η ranges between 0 (2D dipole) and 1 (resp(–1)) (1D

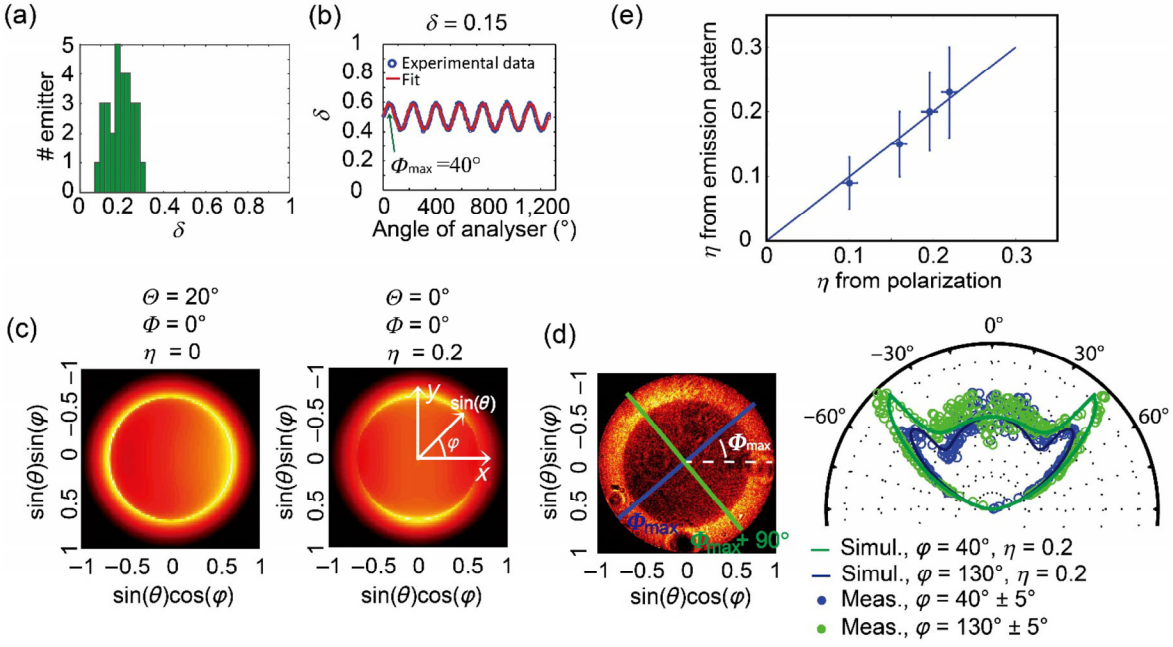

Figure 3 (a) Histogram of measured degree of polarization for 29 different rectangular nanoplatelets deposited on gold substrate. (b) Measured emission polarization curve for a rectangular nanoplatelet. (c) Calculated radiation pattern for a 2D dipole: symmetric dipole with $\eta = 0$ tilted by $\Theta = 30°$ (left), asymmetric dipole with $\eta = 0.2$ and $\Theta = 0°$ (right). (d) Experimental Fourier plane image (left) and radiation pattern (right) of the same rectangular nanoplatelet, and theoretical radiation pattern in the main directions for a 2D asymmetric dipole ($\eta = 0.2$ and $\Theta = 0°$, d_x, with the largest dipole having an orientation making an angle Φ_{max} in the x direction) in the former experimental configuration. (e) Comparison between the dipolar asymmetry η obtained from polarimetry and radiation pattern measurement.

dipole along x (resp(y)). In that case, for a horizontal dipole ($\Theta = 0°$), it can be shown (see the ESM) that the theoretical degree of polarization is proportional to the dipolar asymmetry η.

In the configuration that was just considered (emitter close to gold interface, embedded in semi-infinite 1.45 index media and oil objective), hypotheses (i) and (ii) lead to very similar radiation patterns (not shown here). However, the difference between these two cases appears clearly (Fig. 3(c)) when the gold-silica substrate is replaced by a glass substrate, with the nanoplatelets lying on the air side of the interface, so that the oil objective collects leakage radiation (see Fig. S1 in the ESM). In the first case (i) (asymmetric dipole with $\eta = 0.2$ and $\Theta = 0°$), the theoretical Fourier image (Fig. 3(c), right) shows a sharp ring at the air-glass critical angle, with a symmetric saddle shape and two opposite lobes. In contrast, in hypothesis (ii) (tilted dipole, $\eta = 0$ and $\Theta = 20°$) (Fig. 3(c), left), the ring is mostly isotropic, but the emission at the critical angle show a slight dissymmetry. In this configuration, the radiation pattern raises the possibility of discriminating between the two hypotheses: (i) asymmetric dipole ($\Theta = 0$ and $\eta \neq 0$) and (ii) tilt of the 2D dipole ($\eta = 0$ and $\Theta \neq 0$).

For the same rectangular nanoplatelets, we perform polarimetric emission pattern experiments. Figure 3(b) plots a typical $I(\alpha)$ polarimetry curve. The measured degree of polarization is 0.15, and can indicate (depending on which hypothesis we make) either that $\eta = 0$ and $\Theta = 30°$ (tilted dipole), or that $\eta = 0.2$ and $\Theta = 0°$. Figure 3(d) shows the measured radiation pattern for the same rectangular nanoplatelet. The pattern is in qualitative agreement with the theoretical pattern for an asymmetric dipole, and not with the pattern for a tilted dipole. The theoretical radiation pattern along the main axes ($\varphi = \Phi_{max}$ and $\varphi = \Phi_{max} + \pi/2$ with Φ_{max} being the in-plane dipole orientation extracted from polarization measurements, as shown in Fig. 3(d)) even shows excellent quantitative agreement with the experimental data by considering a dipolar asymmetry $\eta = 0.2$. Therefore, the radiation pattern is described by an asymmetric dipole, thereby excluding the tilted dipole hypothesis.

In another set of experiments (Fig. S4 in the ESM), we use several nanoplatelets to confirm the correlation between polarized emission and asymmetric emission patterns, and outline that correlation using the dipolar asymmetry factor η. For each nanoplatelet, the value of η can be extracted from the radiation, pattern by fitting the radiation pattern with the theoretical curve ($\Theta = 0°$, $\varphi = \Phi_{max}$, $\eta \neq 0$). This value of η is compared to the value obtained from the polarimetry analysis. As shown in Fig. 3(e), both polarimetry and radiation pattern measurements produce very similar values, which confirms the validity of the asymmetric 2D-dipole model for describing rectangular nanoplatelet emission. For different rectangular nanoplatelets, values of η ranging from 0.1 to 0.25 are measured.

In conclusion, we demonstrated a correlation between nanoplatelet shape anisotropy (τ) and dipolar asymmetry (η). Rectangular nanoplatelets exhibited polarized emission and asymmetric emission patterns, whereas square nanoplatelets exhibited nonpolarized emission and symmetric emission patterns.

3.3 Origins of emission asymmetry for rectangular platelets

For all fluorescent semiconductor nanostructures, the emitting dipole reflects the symmetries and oscillator strengths of the radiating electron–hole pair states confined inside the structure. These can be modeled by quantum mechanics calculations. However, for nanoplatelets at room temperature, lateral confinement effects are negligible [20], because the lateral confinement energy is much lower than $k_B T$. The electron–hole states are only confined in the vertical direction, and their dipolar nature should not be influenced by the lateral aspect ratio of the platelets. A second effect that can influence the emission is an optical effect, because the structures (both core and shell) act as a dielectric antenna that can modify both radiation patterns and polarization. This effect is particularly strong if there is a large contrast between the dielectric constants and the environment outside the structure, as is the case here. Electric field modifications can then be highly nonuniform when a structure is not isotropic, and there is no simple analytical equation to describe this effect [33]. Nevertheless, in the former section, we modeled the emission of rectangular nanoplatelets by a point-like 2D-asymmetric dipole, without considering any lateral embedding dielectric media. We have

therefore assumed that the antenna dielectric effect that enhances the emitted field in a specific direction can be mimicked by a larger dipolar contribution in that direction, and therefore to an asymmetric dipole. In this last section, we discuss the validity of this assumption, and consider a point-like radiating dipole embedded in a dielectric structure, with the dimensions of a platelet and with a dielectric index corresponding to a bulk CdSe platelet.

For this objective, we compare the radiation pattern in two cases: a 2D symmetric dipole in a rectangular nanoplatelet and a 2D asymmetric dipole in a square nanoplatelet. For this part, in contrast to the previous analytical simulation of the radiation pattern, we use a finite element numerical method to simulate the radiation patterns of a 2D dipole embedded in a square or rectangular nano-object and having a dielectric index equal to 2.588. Thus, for emission pattern simulations, we take into account the lateral confinement caused by the dielectric contrast between the nanoplatelet and its environment.

Both the nano-objects and dipoles lie on the air side of a glass–air interface (Θ = 0°). The dipolar emission is collected in the glass half-space. The symmetric dipole (η = 0) is embedded within a rectangular nano-object of dimensions 20 nm × 15 nm × 2 nm, as measured by TEM on the rectangular platelets (Fig. 4(b)), whereas the 2D asymmetric dipole (η = 0.2) is inside a square nano-object (15 nm × 15 nm × 2 nm) (Fig. 4(a)).

For the asymmetric dipole in the square nanoplatelet, the stronger dipole along the X-axis (Φ = 0°) induces stronger emission in the Y direction (φ = 90°, see Fig. 3(d)). With respect to the symmetric dipole in a rectangular nanoplatelet (Fig. 4(b)), the dielectric antenna effect from the elongated shape along the X axis of the nanoplatelet induces a field distribution inside the nanoplatelet along the X axis, as well as the additional confinement of the Y axis. Therefore, in the far field, emission is enhanced in the Y direction.

Emission asymmetries are very similar in the two cases, leading to the conclusion that the asymmetric emission of a rectangular nanoplatelet can be modeled with excellent quantitative agreement, either as an asymmetric 2D dipole ($d_x \neq d_y$) without considering any embedding medium (as stated in the beginning of the paper), or as a 2D symmetric dipole within a rectangular nano-object of finite size. However, because the lateral size of the nanoplatelets is much larger than the dimensions for lateral electron–hole confinement, the 2D dipole is not sensitive to lateral nanoplatelets size, and must be considered as a 2D symmetric dipole. Therefore, emission asymmetry can be appropriately described quantitatively by the dielectric antenna effect induced by the elongated shape of a rectangular nano-object.

Finally, we performed similar numerical simulations (Figs. S2 and S3 in the ESM) with different platelet dielectric constants and lengths. We found that by increasing rectangular platelet length while maintaining width at 15 nm, emission asymmetry in the radiation pattern increases. Emission asymmetry is also found to increase as a function of the platelet index.

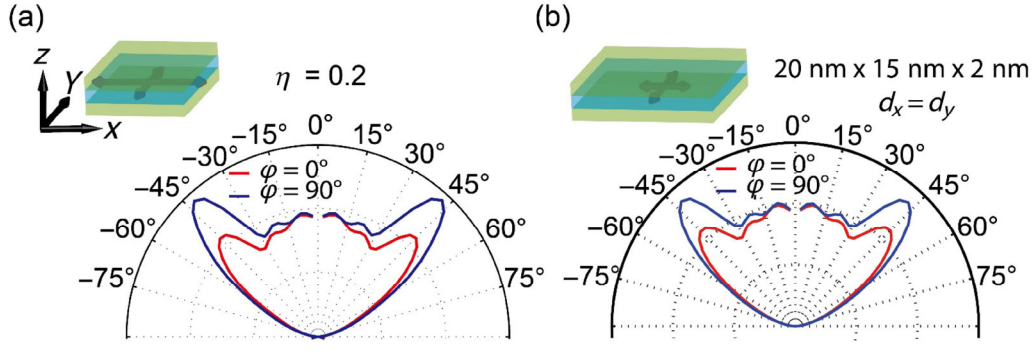

Figure 4 Simulated radiation patterns for emission along x direction φ = 0° (red curve) and y-direction φ = 90° (blue curve). The index of the nanoplatelets is taken equal to 2.588 (a) 2D asymmetric dipole with factor η = 0.2 ($d_x > d_y$) in a square nanoplatelet; (b) 2D symmetric dipole in a rectangular nanoplatelet.

4 Conclusion

In conclusion, we demonstrate in this study that rectangular nanoplatelets exhibit asymmetric emission behavior (polarization and radiation patterns), while the emission of square nanoplatelets remains isotropic. We characterize the dipolar nature of the emission by combining polarimetry and radiation pattern measurements, and by choosing different substrates, to emphasize the different effects that will be analyzed. We showed that the emission of individual square nanoplatelets is nonpolarized and well described by a 2D dipole, which always lies horizontally on the substrate. In contrast, a rectangular nanoplatelet exhibits more polarized emission, and its radiation patterns become asymmetric. Both aspects can be modeled in a first step with good quantitative agreement by mimicking rectangular nanoplatelets as asymmetric 2D dipoles ($d_x \neq d_y$) whose dipolar asymmetry factors (η values) range from 0.1 to 0.2. In a second step, numerical simulations show that this emission asymmetry can be well explained by the anisotropic shape of the platelet, which acts as a dielectric nanoantenna for the emission of a symmetric 2D dipole. A correlation is thus evidenced between the geometric aspect ratio of colloidal nanoplatelets and the asymmetric properties of their fluorescence emission.

The combination of radiation pattern and polarimetry analyses is a powerful characterization method for studying the dipolar nature of single objects, which allows for a detailed understanding of fluorescent nanostructures, and illustrates the different contributions of electron–hole confinement and dielectric antenna effects on overall emission properties.

Acknowledgements

This work was supported by the Agence Nationale de la Recherche (project JCJC 12-JS04-0011-01 PONIMI), the Centre de Compétence Nanosciences Ile-de-France (Patch project) and by the CNRS program Platon (PICS 6456). Among their co-workers at INSP, the authors would like to thank Catherine Schwob and Jean-Marc Frigerio for fruitful discussions, Willy Daney de Marcillac for his help on the microscopy setup, Francis Breton for the setup interface and Loïc Becerra and Mélanie Escudier for the substrate preparation.

References

[1] Empedocles, S. A.; Neuhauser, R.; Bawendi, M. G. Three-dimensional orientation measurements of symmetric single chromophores using polarization microscopy. *Nature* **1999**, *399*, 126–130.

[2] Chung, I.; Shimizu, K. T.; Bawendi, M. G. Room temperature measurements of the 3D orientation of single CdSe quantum dots using polarization microscopy. *Proc. Natl. Acad. Sci. USA* **2003**, *100*, 405–408.

[3] Brokmann, X.; Coolen, L.; Dahan, M.; Hermier, J. P. Measurement of the radiative and nonradiative decay rates of single CdSe nanocrystals through a controlled modification of their spontaneous emission. *Phys. Rev. Lett.* **2004**, *93*, 107403.

[4] Lethiec, C.; Laverdant, J.; Vallon, H.; Javaux, C.; Dubertret, B.; Frigerio, J. M.; Schwob, C.; Coolen, L.; Maître, A. Measurement of three-dimensional dipole orientation of a single fluorescent nanoemitter by emission polarization analysis. *Phys. Rev. X* **2014**, *4*, 021037.

[5] Cassette E.; Mahler, B.; Guigner, J. M.; Patriarche, G.; Dubertret, B.; Pons, T. Colloidal CdSe/CdS dot-in-plate nanocrystals with 2D-polarized emission. *ACS Nano* **2012**, *6*, 6741–6750.

[6] Chen, X.; Nazzal, A.; Goorskey, D.; Xiao, M.; Peng, Z. A.; Peng, X. G. Polarization spectroscopy of single CdSe quantum rods. *Phys. Rev. B* **2001**, *64*, 245304.

[7] Lethiec, C.; Pisanello, F.; Carbone, L.; Bramati, A.; Coolen, L.; Maître, A. Polarimetry-based analysis of dipolar transitions of single colloidal CdSe/CdS dot-in-rods. *New J. Phys.* **2014**, *16*, 093014.

[8] Cyphersmith, A.; Early, K.; Maksov, A.; Graham, J.; Wang, Y.; Barnes, M. Disentangling the role of linear transition dipole in band-edge emission from single CdSe/ZnS quantum dots: Combined linear anisotropy and defocused radiation pattern imaging. *Appl. Phys. Lett.* **2010**, *97*, 121915.

[9] Vezzoli, S.; Manceau, M.; Leménager, G.; Glorieux, Q.; Giacobino, E.; Carbone, L.; De Vittorio, M.; Bramati, A. Exciton fine structure of CdSe/CdS nanocrystals determined by polarization microscopy at room temperature. *ACS Nano* **2015**, *9*, 7992–8003.

[10] Hadar, I.; Hitin, G. B.; Sitt, A.; Faust, A.; Banin, U. Polarization properties of semiconductor nanorod hetero-structures: From single particles to the ensemble. *J. Phys. Chem. Lett.* **2013**, *4*, 502–507.

[11] Sitt, A.; Salant, A.; Menagen, G.; Banin, U. Highly emissive nano rod-in-rod heterostructures with strong linear polarization. *Nano Lett.* **2011**, *11*, 2054–2060.

[12] Diroll, B. T.; Dadosh, T.; Koschitzky, A.; Goldman, Y. E.; Murray, C. B. Interpreting the energy-dependent anisotropy of colloidal nanorods using ensemble and single-particle spectroscopy. *J. Phys. Chem. C* **2013**, *117*, 23928–23937.

[13] Shan, C. X.; Liu, Z.; Hark, S. K. Photoluminescence polarization in individual CdSe nanowires. *Phys. Rev. B* **2006**, *74*, 153402.

[14] Kovalev, D.; Averboukh, B.; Ben-Chorin, M.; Koch, F.; Efros, A. L.; Rosen, M. Optically induced polarization anisotropy in porous Si. *Phys. Rev. Lett.* **1996**, *77*, 2089–2092.

[15] Ithurria, S.; Tessier, M. D.; Mahler, B.; Lobo, R. P. S. M.; Dubertret, B.; Efros, A. L. Colloidal nanoplatelets with two-dimensional electronic structure. *Nat. Mater.* **2011**, *10*, 936–941.

[16] Mahler, B.; Nadal, B.; Bouet, C.; Patriarche, G.; Dubertret, B. Core/shell colloidal semiconductor nanoplatelets. *J. Am. Chem. Soc.* **2012**, *134*, 18591–18598.

[17] Pelton, M.; Ithurria, S.; Schaller, R. D.; Dolzhnikov, D. S.; Talapin, D. V. Carrier cooling in colloidal quantum wells. *Nano Lett.* **2012**, *12*, 6158–6163.

[18] Joo, J.; Son, J. S.; Kwon, S. G.; Yu, J. H.; Hyeon, T. Low-temperature solution-phase synthesis of quantum well structured CdSe nanoribbons. *J. Am. Chem. Soc.* **2006**, *128*, 5632–5633.

[19] Ithurria, S.; Dubertret, B. Quasi 2D colloidal CdSe platelets with thicknesses controlled at the atomic level. *J. Am. Chem. Soc.* **2008**, *130*, 16504–16505.

[20] Tessier, M. D.; Javaux, C.; Maksimovic, I.; Loriette, V.; Dubertret, B. Spectroscopy of single CdSe nanoplatelets. *ACS Nano* **2012**, *6*, 6751–6758.

[21] Hines, M. A.; Guyot-Sionnest, P. Synthesis and characterization of strongly luminescing ZnS-capped CdSe nanocrystals. *J. Phys. Chem.* **1996**, *100*, 468–471.

[22] Reiss, P.; Protière, M.; Li, L. Core/shell semiconductor nanocrystals. *Small* **2009**, *5*, 154–168.

[23] de Mello Donegá, C. Synthesis and properties of colloidal heteronanocrystals. *Chem. Soc. Rev.* **2011**, *40*, 1512–1546.

[24] Mahler, B.; Spinicelli, P.; Buil, S.; Quelin, X.; Hermier, J.-P.; Dubertret, B. Towards non-blinking colloidal quantum dots. *Nat. Mater.* **2008**, *7*, 659–664 .

[25] Chen, Y. F.; Vela, J.; Htoon, H.; Casson, J. L.; Werder, D. J.; Bussian, D. A.; Klimov, V. I.; Hollingsworth, J. A. "Giant" multishell CdSe nanocrystal quantum dots with suppressed blinking. *J. Am. Chem. Soc.* **2008**, *130*, 5026–5027.

[26] Biadala, L.; Liu, F.; Tessier, M. D.; Yakovlev, D. R.; Dubertret, B.; Bayer, M. Recombination dynamics of band edge excitons in quasi-two-dimensional CdSe nanoplatelets. *Nano Lett.* **2014**, *14*, 1134–1139.

[27] Olutas, M.; Guzelturk, B.; Kelestemur, Y.; Yeltik, A.; Delikanli, S.; Demir, H. V. Lateral size-dependent spontaneous and stimulated emission properties in colloidal CdSe nanoplatelets. *ACS Nano* **2015**, *9*, 5041–5050.

[28] She, C. X.; Fedin, I.; Dolzhnikov, D. S.; Dahlberg, P. D.; Engel, G. S.; Schaller, R. D.; Talapin, D. V. Red, yellow, green, and blue amplified spontaneous emission and lasing using colloidal CdSe nanoplatelets. *ACS Nano* **2015**, *9*, 9475–9485.

[29] Achtstein, A. W.; Scott, R.; Kickhöfel, S.; Jagsch, S. T.; Christodoulou, S.; Bertrand, G. H. V.; Prudnikau, A. V.; Antanovich, A.; Artemyev, M.; Moreels, I.; Schliwa, A.; Woggon, U. p-State luminescence in CdSe nanoplatelets: Role of lateral confinement and a longitudinal optical phonon bottleneck. *Phys. Rev. Lett.* **2016**, *116*, 116802.

[30] Cunningham, P. D.; Souza, J. B. Jr.; Fedin, I.; She, C. X.; Lee, B.; Talapin, D. V. Assessment of anisotropic semiconductor nanorod and nanoplatelet heterostructures with polarized emission for liquid crystal display technology. *ACS Nano* **2016**, *10*, 5769–5781.

[31] Beaudoin, E.; Abecassis, B.; Constantin, D.; Degrouard, J.; Davidson, P. Strain-controlled fluorescence polarization in a CdSe nanoplatelet-block copolymer composite. *Chem. Commun.* **2015**, *51*, 4051–4054.

[32] Gippius, N. A.; Tikhodeev, S. G.; Kulakovskiĭ, V. D.; Forchel, A. Optical polarization effects in semiconductor/vacuum nanostructures. *JETP Lett.* **1994**, *59*, 556–559.

[33] Rodina, A. V.; Efros, A. L. Effect of dielectric confinement on optical properties of colloidal nanostructures. *J. Exp. Theor. Phys.* **2016**, *122*, 554–566.

[34] Tessier, M. D.; Mahler, B.; Nadal, B.; Heuclin, H.; Pedetti, S.; Dubertret, B. Spectroscopy of colloidal semiconductor core/shell nanoplatelets with high quantum yield. *Nano Lett.* **2013**, *13*, 3321–3328.

[35] Bouet, C.; Mahler, B.; Nadal, B.; Abecassis, B.; Tessier, M. D.; Ithurria, S.; Xu, X. Z.; Dubertret, B. Two-dimensional growth of CdSe nanocrystals, from nanoplatelets to nanosheets. *Chem. Mater.* **2013**, *25*, 639–645.

[36] Pelliser, L.; Manceau, M.; Lethiec, C.; Coursault, D.; Vezzoli, S; Leménager, G.; Coolen, L.; DeVittorio, M.; Pisanello, F.; Carbone, L. et al. Alignment of rod-shaped single-photon emitters driven by line defects in liquid crystals. *Adv. Funct. Mater.* **2015**, *25*, 1719–1726.

[37] Lukosz, W. Light emission by magnetic and electric dipoles close to a plane dielectric interface. III. Radiation patterns of dipoles with arbitrary orientation. *J. Opt. Soc. Am.* **1979**, *69*, 1495–1503.

[38] Novotny, L. *Principles of Nano-Optics*; Cambridge University Press: Cambridge, 2006.

[39] Chuang, S. L. *Physics of Optoelectronic Devices*; Wiley-Interscience: New York, 1995.